Joint estimation of frequency offset and chromatic dispersion based on the training sequences in M-ary QAM coherent optical transmission system

Yiping Sun (孙艺萍)[1], Lixia Xi (席丽霞)[1*], Xianfeng Tang (唐先锋)[1], Donghe Zhao (赵东鹤)[1], Yaojun Qiao (乔耀军)[1], Xia Zhang (张 霞)[1,2], and Xiaoguang Zhang (张晓光)[1]

[1]*State Key Laboratory of Information Photonics and Optical Communications, Beijing University of Posts and Telecommunications, Beijing 100876, China*

[2]*The Key Laboratory of Optical Communications Science & Technology in Shandong Province, Liaocheng University, Liaocheng 252000, China*

[*]*Corresponding author: xilixia@bupt.edu.cn*

Received April 16, 2014; accepted July 16, 2014; posted online Month September 29, 2014

A data-aided method of joint frequency offset and chromatic dispersion estimation based on the Chu training sequences is shown in 112 Gb/s polarization-multiplexed (PM) quadrature phase-shift keying and 224 Gb/s PM-16-quadrature amplitude modulation with different pulse-shaping filters, respectively. The proposed method achieves a good accuracy and is verified to be robust to polarization mode dispersion.

OCIS codes: 060.1660, 060.2330, 060.4510.

DOI: 10.3788/COL201412.100606.

Nowadays, the focus of next-generation optical networks is moving beyond 100 Gb/s[1], and coherent detection together with digital signal processing (DSP) is adopted for the high-speed optical networks due to their excellent performance in the system[2,3]. In coherent optical transmission system, accurate chromatic dispersion (CD) estimation is vital because both the timing recovery and the channel equalization are based on the success of CD monitoring[4,5]. Data-aided (DA) channel estimation is one of the many techniques of CD estimation, which is a promising solution for the high-speed optical transmission system. The DA method uses the training sequences (TSs), which make the estimation faster and more robust. However, DA channel estimation is susceptible to the frequency offset caused by the frequency mismatch between the transmitter laser and the local oscillator (LO)[6]. Thus, precise estimation of frequency offset needs to be conducted before the channel estimation[7,8].

DA technique can estimate both the CD and the polarization mode dispersion (PMD) impairments[9,10] through the channel transfer function. The transfer function is usually obtained using TSs such as Golay sequences[11] and constant amplitude zero autocorrelation (CAZAC) Chu sequences[12]. However, this DA technique can only be carried out after the frequency offset is successfully compensated. Generally, frequency offset estimation can be done by using either DA or blind method. One method mitigates the frequency offset and phase noise with the aid of pilot symbols[13], which may cost extra symbols. Another method using the periodicity of repeated TSs is proposed to realize frame synchronization, frequency offset estimation, and channel estimation simultaneously, which could require a relatively big overhead[14]. Blind frequency offset estimation[15] is also widely used, but it may be a bit slow on convergence speed compared to the DA method.

In this letter, joint estimation of frequency offset and CD based on TSs is realized through the channel transfer function. Only two CAZAC Chu sequences need to be generated to calculate the transfer function. This combined estimation method is shown with good accuracy and wide estimation range for both polarization-multiplexed quadrature phase-shift keying (PM-QPSK) and PM-16-quadrature amplitude modulation (PM-16-QAM) coherent systems. Its independence of pulse-shaping filters and tolerance to PMD are also investigated.

CAZAC Chu sequences[12] are composed of complex codes, which are widely used for channel estimation based on their correlation property. Assuming a set of code $\{a_k\}$ of length N satisfies the Chu sequences formation[12]:

$$a_k = \begin{cases} \exp \mathrm{i}\dfrac{M\pi k^2}{N}, & \text{when } N \text{ is even} \\ \exp \mathrm{i}\dfrac{M\pi k(k+1)}{N}, & \text{when } N \text{ is odd} \end{cases}, \quad (1)$$

where $k = 0, 1, 2, \ldots, N-1$ indicates the sequence number of the code and M is an integer that is prime to N. Different sequences with the same length can be derived by giving different values to M and they are orthogonal to each other. We choose to use two Chu sequences b_k and c_k, both of which have the same length and arrange them as Alamouti scheme[16] to do the channel estimation. However, the elements of the original Chu sequences stay around the unit circle, which is shown in Fig. 1(a). To satisfy the format of the transmission system and make the code customize for the modulator, we transform the original sequences through a QPSK or 16-QAM slicer. The Chu sequences after QPSK slicer, b_k' and c_k', are mathematically formulated as

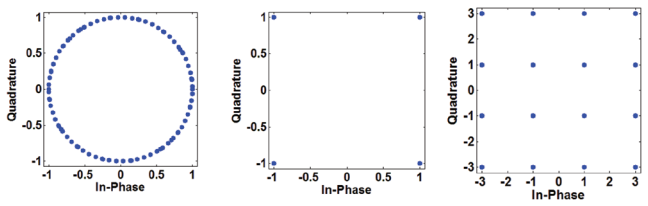

(a) (b) (c)

Fig. 1. Constellation diagram of (a) original CAZAC Chu sequence, (b) QPSK Chu sequence, and (c) 16-QAM Chu sequence.

$$b_k' = \mathrm{sgn}(\mathrm{real}(b_k)) + \mathrm{j} * \mathrm{sgn}(\mathrm{imag}(b_k)), \quad (2)$$

$$c_k' = \mathrm{sgn}(\mathrm{real}(c_k)) + \mathrm{j} * \mathrm{sgn}(\mathrm{imag}(c_k)), \quad (3)$$

where sgn equals to 1 if the variable is bigger than 0 and −1 if it is smaller than 0. The 16-QAM slicer is designed based on the QPSK sliced code, the codes b_k'' and c_k'' after 16-QAM slicer are shown as

$$b_k'' = 2 * b_k' + c_k', \quad (4)$$

$$c_k'' = -2 * c_k' + b_k', \quad (5)$$

The distributions of the codes after the slicer are shown in Figs. 1(b) and (c). Then we used the sliced Chu sequences for CD and frequency offset estimation. Although the constant amplitude and zero autocorrelation of the sequences are not ideal anymore, they do not cause the degradation in the estimation performance.

The transmission channel based on the TSs can be modeled as[17]

$$\begin{pmatrix} R_X[k] \\ R_Y[k] \end{pmatrix} = \begin{pmatrix} H_{XX}[k] & H_{XY}[k] \\ H_{YX}[k] & H_{YY}[k] \end{pmatrix} \begin{pmatrix} S_X[k] \\ S_Y[k] \end{pmatrix} + \begin{pmatrix} n_X[k] \\ n_Y[k] \end{pmatrix}, \quad (6)$$

where $R_X[k]$ and $R_Y[k]$ are the elements on the X and Y polarizations of the received matrix $\mathbf{R}[k]$; $H_{XX}[k]$, $H_{YX}[k]$, $H_{XY}[k]$, and $H_{YY}[k]$ are the elements of the channel transfer matrix $\mathbf{H}[k]$; $S_X[k]$ and $S_Y[k]$ are the elements on the X and Y polarizations of the transmitted matrix $\mathbf{S}[k]$; $n_X[k]$ and $n_Y[k]$ are the noise elements on the two polarizations. The constructed Chu sequences are sent with the data information in the transmitter side, and then the transmitted matrix $\mathbf{S}[k]$ is modeled as the unitary matrix that has the form[17]:

$$\mathbf{S}[k] = \begin{pmatrix} S_X[k] \\ S_Y[k] \end{pmatrix} = \begin{pmatrix} B[k], -C[k]^* \\ C[k], B[k]^* \end{pmatrix}. \quad (7)$$

If we ignore the influence of noise, the channel transfer matrix $\mathbf{H}[k]$ can be derived by multiplying the inverse of the transmitted matrix in the receiver:

$$\mathbf{H}[k] \approx \mathbf{R}[k]\mathbf{S}[k]^{-1}. \quad (8)$$

As we all know, the CD matrix can be modeled as $H_{\mathrm{CD}}(f) = \exp(-\mathrm{j}f^2(\pi\lambda_0{}^2 Dz/c))$, where λ_0 is the center wavelength, D the fiber dispersion parameter, z the transmission length, and c the speed of light[18]. For the frequency offset, it is modeled as a complex multiplicative distortion of the signal in the time domain $e^{\mathrm{j}*2\pi\Delta ft}$, where Δf denotes the frequency difference between the transmitter and receiver oscillators[19]. The transfer matrix $\mathbf{H}(f)$ changes to $\mathbf{H}(f+\Delta f)$ after it convolves with the frequency offset $\delta(f+\Delta f)$ in the frequency domain. Thus, the transfer matrix contains the information of CD as well as frequency offset. According to the properties of the transfer matrix[17], we calculate the angle of the square root of its determinant,

$$\begin{aligned} \arg\left(\sqrt{\det(\mathbf{H}(f+\Delta f))}\right) &= (f+\Delta f)^2 \frac{\pi D\lambda_0^2 z}{c} \\ &= \left(f^2 + 2\Delta f\, f + \Delta f^2\right)\frac{\pi D\lambda_0^2 z}{c} \\ &= Ef^2 + Ff + G, \end{aligned} \quad (9)$$

then the product of D and z, which represents the value of CD, and Δf, which represents the frequency offset, can be estimated by the quadratic function in Eq. (9).

A 112-Gb/s QPSK and 224-Gb/s 16-QAM coherent transmission system is set up (shown in Fig. 2) to verify the correctness and efficiency of our joint frequency offset and CD estimation method. In the transmitter side, the generated Chu sequences transmit with the information data, which are shaped by NRZ pulse-shaping filters, and then the sequences are modulated to the X and Y polarizations. A PMD emulator (PMDE) and standard single-mode fiber are used to generate differential group delay (DGD) and CD, where DGD represents for the value of PMD. Optical signal-to-noise ratio (OSNR) is generated by erbium-doped fiber amplifier (EDFA) and controlled through the attenuator. Thus, the effect of PMD and OSNR to the performance of CD and frequency offset estimation can be analyzed. In the receiver side, the frequency offset is realized by tuning the frequency of the LO. Then, the sequences are received by the coherent polarization diversity optical receiver, and the analog-to-digital converter (ADC) module oversamples the received signal for two samples per symbol. A perfect clock recovery is assumed and then we can estimate the value of CD as well as frequency offset in the offline DSP module.

The frame of the sequences is shown in Fig. 3. Two orthogonal Chu TSs are used on each polarization, every sequence with length of 128/256-symbol. Figure 4(a) shows the CD estimation curve for 1000-km PM-QPSK transmission system, and the CD as well as frequency offset estimation curve is shown in Fig. 4(b) with blue solid line being the estimated line after data fitting. The black dashed line is theoretical and the red short dashed line is the estimated curve before data fitting. It should be noted that the zero frequency in Fig. 4 corresponds to the frequency of the optical signal with the center wavelength 1550 nm. The blue solid line is

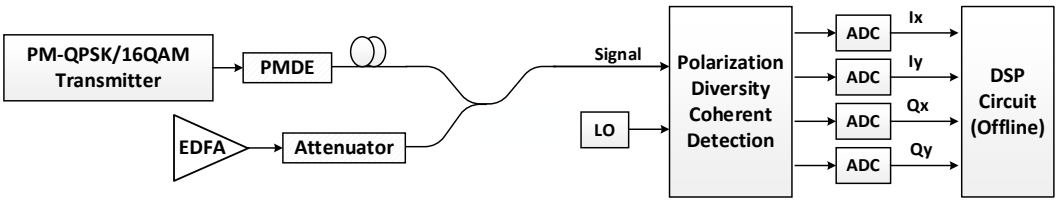

Fig. 2. Architecture of the PM-QPSK/16QAM coherent transmission system

X-polarization	B	-C*
Y-polarization	C	B*

Fig. 3. Frame of the sequences.

assumed to be a quadratic function that has the form: $y = Ex^2 + Fx + G$, then frequency offset Δf equals to $F/2E$ and CD parameter Dz equals to $Ec / \pi\lambda_0^2$ according to Eq. (9).

To check the performance of CD estimation using the proposed method, the estimated CD value and root-mean-square (RMS) estimation error against true CD value for QPSK and 16-QAM formats with different sequence lengths N is presented in Fig. 5 and the relative simulation parameters are given in Table 1. We can observe that the sequence with longer length has better performance compared to the shorter one, because it provides more data for the quadratic interpolation. The method always has a worst-case estimation error around ±200 ps/nm overall the range of 3000–30000 ps/nm for both QPSK and 16-QAM formats. In addition, this method is also valid for the case of small CD value. The estimation performance is also good in both QPSK and 16-QAM systems. The absolute value of the estimation error is always below 70 ps/nm.

We then investigate the performance of frequency offset estimation in the QPSK and 16-QAM transmission systems. Figure 6 shows the estimated value and the RMS estimation error with different sequence lengths N against true value of frequency offset. The estimation performance is better by using the longer TS. The worst-case estimation error of frequency offset is around ±0.1 GHz with a sequence length of 256 in both QPSK and 6-QAM transmission systems.

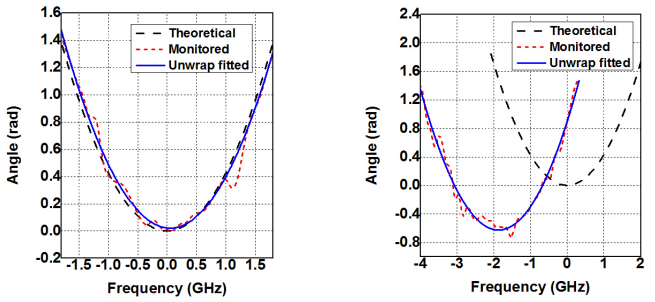

Fig. 4. Data fitting results of (a) CD estimation and (b) joint CD and frequency offset estimation with frequency offset = 2 GHz for QPSK 1000-km transmission.

Table 1. Simulation Parameters

Impairments	Value Range
CD (ps/nm)	3400–30600
Frequency Offset (GHz)	−5 to 5
OSNR (dB)	30
DGD (ps)	0–40
Polarization Angle (rad)	$\pi/4$

We also consider the performance of the proposed estimation method against different pulse-shaping filters. Besides the NRZ pulse shape that has been used for the simulation, other three pulse shapes RZ-33, RZ-50, and RZ-67 are used before the TSs, which are modulated in QPSK transmission system with a sequence length of 256. Figure 7 shows the RMS estimation error of CD and frequency offset against different pulse shapes. Simulation results show that the proposed method can still estimate the value of CD and frequency offset with the other pulse shapes and they always achieve very good accuracy.

Further, we evaluate the CD and frequency offset estimation in the presence of first-order PMD. In the simulation, the transmission distance is set to 1200-km. Figure 8 shows the RMS error percentage of the estimated CD and frequency offset with the DGD value from 0 to 40 ps with different sequence lengths for QPSK and 16-QAM transmission systems, where the error

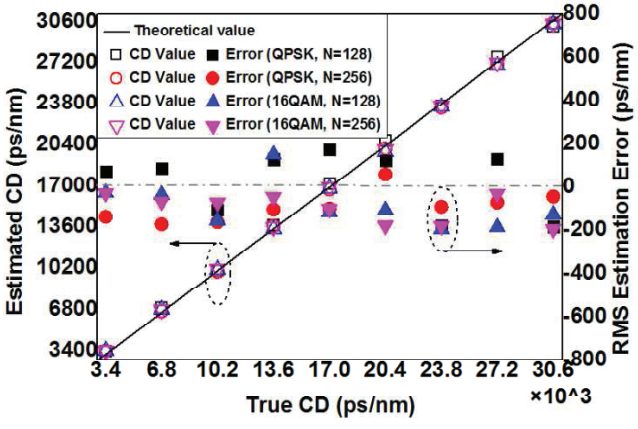

Fig. 5. Estimated CD value and the RMS estimation error versus true CD with different sequence lengths for QPSK and 16-QAM transmission systems with frequency offset = 0 GHz.

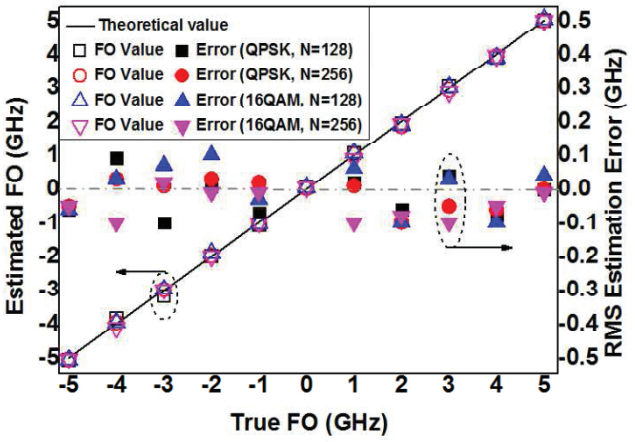

Fig. 6. Estimated value and the RMS estimation error of frequency offset versus true frequency offset with different sequence lengths for QPSK and 16-QAM over 1200-km transmission.

percentage is defined as the absolute value of the relative error. It can be seen that the CD estimation performance degrades as the value of DGD increases, but still reaches an estimation error percentage lower than 4%. At the same time, the performance of frequency offset estimation is slightly influenced by DGD. With the sequence length of 256, the error rate is always below 1% in presence of first-order PMD for both the QPSK and 16-QAM systems.

In conlusion, a DA method using the CAZAC Chu sequences is proposed to accurately measure the frequency offset and CD value at the same time. The method is simple and applicable to multiple modulation formats as well as various data rates. We show the method by simulation in 28 Gbaud PM-QPSK and PM-16-QAM transmission systems and find that the estimation performance can be improved by choosing longer Chu sequences. This method realizes an accurate CD and frequency offset estimation over a wide range. For both QPSK and 16-QAM systems with a sequence length of 256, the absolute value of CD estimation error is below 200 ps/nm and the absolute value of frequency offset estimation error is less than 0.1 GHz. Furthermore, the

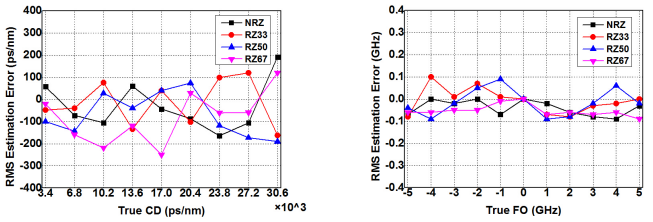

Fig. 7. RMS Estimation Error of (a) CD and (b) Frequency offset estimation against different pulse shaping filters in QPSK transmission system with a sequence length of 256 over 1200-km transmission (frequency offset = 4GHz).

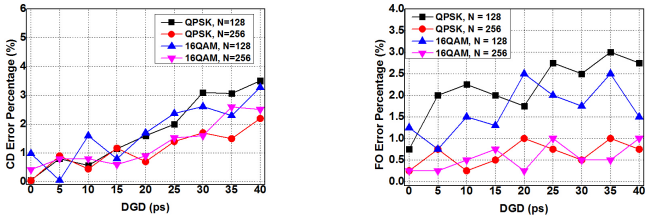

Fig. 8. RMS error percentage of (a) CD estimation and (b) frequency offset estimation against DGD over 1200-km transmission with frequency offset = 4 GHz.

DA method is proved to be insensitive to pulse-shaping filters and robust to PMD.

This work was supported by the National Natural Science Foundation of China (No. 61205065), the National "863" Project of China (No. 2013AA013401), and the Open Fund of State Key Laboratory of optical fiber communication network with the new type of optical communication system (Shanghai Jiao Tong University) (No. 2013GZKF031310).

References

1. P. Winzer, IEEE Commun. **48,** 26 (2010).
2. M. S. Faruk and K. Kazuro, Opt. Express **19,** 12789 (2011).
3. Y. Xu, Y. Qiao, and Y. Ji, Chin. Opt. Lett. **10,** 110601 (2012).
4. C. K. C. Chan, *Optical Performance Monitoring: Advanced Techniques for Next-Generation Photonic Networks* (Academic Press, 2010).
5. Z. Huang, F. Zhang, and Z. Chen, Chin. Opt. Lett. **11,** 060601 (2013).
6. R. Elschner, F. Frey, C. Meuer, J. Fischer, S. Alreesh, C. Schmidt-Langhorst, L. Molle, T. Tanimura, and C. Schubert, Opt. Express 20, 28786. (2012).
7. F. Pittala and J. A. Nossek, in *Proceedings of IPC,* 129 (2013).
8. F. Pittala, Q. Juan, M. Msallem, J. A. Nossek, in *Proceedings of 39th European Conference and Exhibition on IET* 1 (2013).
9. C. Do, A. Tran, C. Zhu, S. Chen, T. Anderson, D. Hewitt, and E. Skafidas, IEEE Photon. J. **4**, 2037 (2012).
10. F. Pittalà, F. Hauske, Y. Ye, N. Gonzalez, and I. Monroy, in *Proceedings of ICTON We.D1.5*, (2011).
11. M. Golay, IRE Trans. Inf. Theory **7**, 82 (1961).
12. D. Chu, IEEE Trans. Inf. Theory **18**, 531 (1972).
13. M. Morsy-Osman, Q. Zhuge, M. Chagnon, X. Xu, and D. Plant, in *Proceedings of OFC/NFOEC 2013 OTu3I.6*, (2013).
14. M. Yan, Z. Tao, T. Takahito, S. Oda, Y. Cao, Y. Zhao, T. Hoshida, and J. Rasmussen, in *Proceedings of ECOC*, 1 (2013).
15. Y. Qiao, Z. Wang, and Y. Ji, Chin. Opt. Lett. **8,** 888 (2010).
16. S. Alamouti, IEEE J. Sel. Areas Commun. **16,** 1451 (1998).
17. F. Hauske, M. Kuschnerov, B. Spinnler, and B. Lankl, J. Lightwave Technol. **27,** 3623 (2009).
18. G. P. Agrawal, *Nonlinear Fiber Optics* (Springer, 2000).
19. J. Van de Beek, M. Sandell, and P. Borjesson, IEEE Trans. Signal Process. **45,** 1800 (1997).